J Comp Physiol A (1999) 184: 361–369

ORIGINAL PAPER

R. H. H. Kröger · M. C. W. Campbell
R. D. Fernald · H.-J. Wagner

Multifocal lenses compensate for chromatic defocus in vertebrate eyes

Accepted: 6 November 1998

Abstract The focal length of the vertebrate eye is a function of wavelength, i.e. the eye suffers from longitudinal chromatic aberration. Chromatic defocus is a particularly severe problem in eyes with high light-gathering ability, since depth of field is small due to a pupillary opening that is large in relation to the focal length of the eye. Calculations show that in such eyes only a narrow spectral band of light can be in focus on the retina. For the major part of the visual spectrum, spatial resolution should be limited by the optics of the eye and far lower than the resolving power achievable by the retinal cone photoreceptor mosaic. To solve this problem, fishes with irises unresponsive to light have developed lenses with multiple focal lengths. Well-focused images are created at the wavelengths of maximum absorbance of all spectral cone types. Multifocal lenses also appear to be present in some terrestrial species. In eyes with mobile irises, multifocal lenses are correlated with pupil shapes that allow all zones of the lens, with different refractive powers, to participate in the imaging process, irrespective of the state of pupil constriction.

Key words Color vision · Chromatic aberration · Spherical aberration · Depth of field · Pupil shape

Abbreviations *LCA* longitudinal chromatic aberration · *LSA* longitudinal spherical aberration · *LWS* long-wave-sensitive · *MWS* middle-wave-sensitive · *SWS* short-wave-sensitive

R.H.H. Kröger (✉) · H.-J. Wagner
Anatomisches Institut, Eberhard-Karls-Universität Tübingen,
Österbergstrasse 3, D-72074 Tübingen, Germany
e-mail: kroeger@anatu.uni-tuebingen.de
Tel.: +49-7071-2973022; Fax: +49-7071-294014

M.C.W. Campbell
School of Optometry, University of Waterloo,
Waterloo, Ontario, Canada N2L 3G1

R.D. Fernald
Neuroscience Program and Department of Psychology,
Stanford University, Stanford, CA 94305, USA

Introduction

The eyes of many fishes and nocturnal terrestrial vertebrates have small *f*-numbers – short focal length relative to pupil diameter – in order to maximize light-gathering ability. In such eyes, depth of field is much smaller than in the human eye. Since in simple optical systems like animal eyes the focal length is a function of the wavelength of light (longitudinal chromatic aberration, LCA), differences in focal length due to LCA should degrade the image to an extent that the spatial resolution of color vision should be very poor. However, many fish species have excellent color vision with several, spectrally widely spaced visual pigments (Bowmaker 1995). Among nocturnal terrestrial species, geckos, for instance, have three spectral cone types (Loew et al. 1996) and thus face similar problems caused by LCA. We analyzed the optics of the eye of *Haplochromis burtoni*, a cichlid fish from Lake Tanganyika, and present data which indicate that the problem of chromatic defocus is solved by multiple focal lengths in the lens. Furthermore, we examined eyes with small *f*-numbers in other vertebrates and found that multifocal lenses appear to be present in a variety of species.

Since the cornea contributes little to the refractive power of the eye underwater (Matthiessen 1886), the focal length and image quality of the fish eye depend primarily on lens optics. The typical fish lens is spherical in shape, has a radial internal symmetry of refractive index and short focal length. In *H. burtoni*, the difference in refractive power due to LCA between the wavelengths of maximum absorbance (λ_{max}) of the long- (LWS, 562 nm) and middle-wave-sensitive (MWS, 523 nm) cone photoreceptors is 3.3 diopters for a lens with a radius of 1 mm; between the λ_{max} of the MWS and short-wave-sensitive (SWS, 455 nm) cones it is 9.3 diopters. Between 455 and 562 nm, the difference in image position would be 63 μm (Fig. 1a; Kröger and Campbell 1996). In cichlids, different cone lengths cannot compensate for LCA, as has been suggested for

other fish species (Eberle 1968), since all cone inner segments are aligned at the external limiting membrane in the light-adapted cichlid retina (Kröger and Wagner 1996) and the entrance aperture of a cone appears to be at the proximal (vitread) portion of the inner segment (He and MacLeod 1998). If the λ_{max} of the MWS cones (523 nm) is in focus, the diameters of the blur circles for the λ_{max} of the LWS and SWS cones would be about 15 and 40 μm, respectively, assuming that the lens is free of aberrations other than LCA. Spatial resolution of the cone mosaic is significantly greater than the resolution implied by these blur circles for all spectral cone types. Throughout the retina of *H. burtoni*, cones occur in relative numbers of 2:2:1 (LWS, MWS, SWS, respectively; Fernald 1981) with spacings between spectrally identical cones of 4–5 μm (Fernald 1983).

Homogeneous lenses with spherical surfaces focus monochromatic light passing through the periphery of the lens at closer distances than paraxial rays (longitudinal spherical aberration, LSA). In many vertebrate (Matthiessen 1882; Campbell and Hughes 1981; Sivak and Kreuzer 1983; Axelrod et al. 1988; Pierscionek and Chan 1989; Pierscionek and Augusteyn 1991; Kröger et al. 1994; Jagger and Sands 1996) and invertebrate (Sivak 1991; Sivak et al. 1994) eyes, refractive index decreases gradually from the center toward the surface of the lens, which reduces aberrations, most notably spherical aberration. The residual LSA may even be reversed (Campbell and Hughes 1981). In *H. burtoni*, the fine structure of the refractive index profile within the lens leads to a complex shape of the LSA (Fig. 1b; Kröger et al. 1994).

Ray-tracing was used to determine how the *H. burtoni* lens focuses monochromatic and white light. The results showed that the lens has multiple focal lengths, each creating a well-focused image at the λ_{max} of a distinct spectral cone type. Such tuning of LSA to LCA and cone absorbances was demonstrated directly in isolated lenses of large individuals of *Aequidens pulcher* (blue acara), a cichlid from South and Central American rivers and lakes. Eccentric infra-red photorefractometry (Schaeffel et al. 1987) was used to search for multifocal lenses in a variety of other vertebrate species.

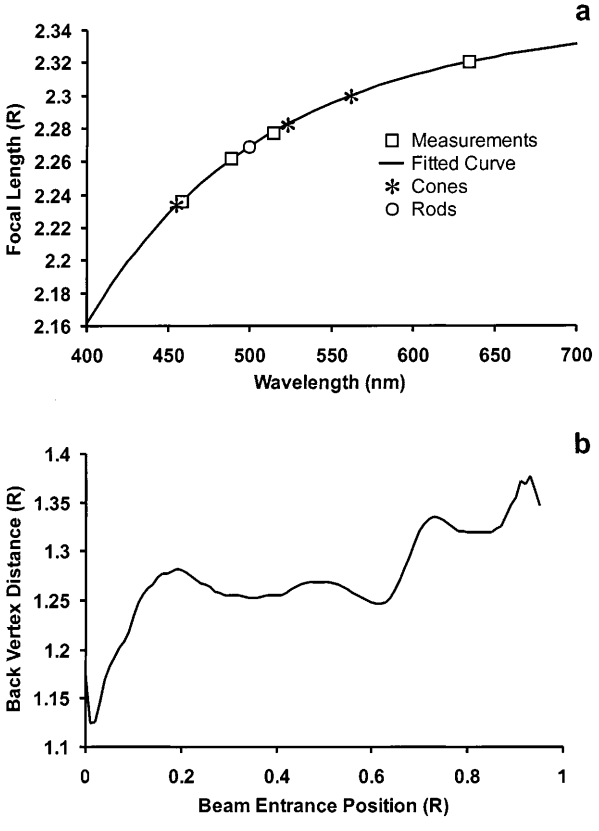

Fig. 1 a The change in the focal length due to longitudinal chromatic aberration (LCA) of the *H. burtoni* crystalline lens. The spectral positions of the λ_{max} of rods and cones are indicated. Data replotted from (Kröger and Campbell 1996). **b** Average longitudinal spherical aberration (LSA) of 21 *H. burtoni* lenses measured at 633 nm. Combined data from Kröger et al. (1994) and Kröger and Campbell (1996)

Materials and methods

The proportions of the cichlid eye, which grows throughout life, are constant if expressed in units of lens radius (Kröger and Fernald 1994). We therefore use the relative unit "*R*" throughout this report since our findings on fish eyes are largely independent of absolute eye and lens size.

Ray-tracing model calculations

To determine the three-dimensional imagery of the fish lens from two-dimensional measurements of LSA, 96 incoming rays with equally spaced entrance positions from 0 to 0.95 *R* were traced to the retina. Most of the light incident on the lens beyond 0.95 *R* is reflected and does not contribute to the image (Sroczynski 1976). Except for the axial ray, each incoming ray represented an annulus of light. The contribution of those rays to retinal illumination therefore was weighted for the area of the corresponding annulus. The point of intercept with the retina of each ray was determined by simple geometry since the trajectories of rays were known from the LSA. On the retina, illumination was calculated by summing the contributions of rays per unit retinal area. Bin width on the retina was 0.0015 *R*, which is about the diameter of the perfect disc of diffraction (e.g., Longhurst 1973). The change in focal length due to LCA was calculated from earlier measurement in the *H. burtoni* lens using laser light of four wavelengths ranging from 457 to 633 nm (Kröger and Campbell 1996). Sources of white light were assumed to have the same power at all wavelengths from 400 to 700 nm. For comparison, calculations were performed for an idealized fish lens with the same color-dispersive properties as the *H. burtoni* lens and with perfectly corrected LSA.

Fish lens imagery

An isolated *A. pulcher* lens with a radius of 1.5 mm was placed on an iris diaphragm and immersed in H10 culture medium (Hikida and Iwata 1987). About 95% of the lens aperture was used for imaging, while stray light passing by the lens was blocked from entering the microscope used for observation. The cones of *A. pulcher* have λ_{max} at 453, 530, and 570 nm (Kröger et al. 1999).

Monochromatic illuminations at spectral positions close to those wavelengths (460, 540, and 580 nm) were produced with interference filters (approx. 5-nm half-maximum bandwidths). As a control, we used a filter with a central wavelength of 480 nm. The target was a back-lit copper grid with bars subtending 2 arcmin,

mesh size was 12 arcmin. A ×40 achromatic water immersion objective with a numerical aperture of 1.2 (Zeiss) was used to view the images created by the lens. Since the numerical aperture of the fish lens was about 0.8, it limited the effective aperture of the fish lens-microscope objective optical system. The focal setting of the microscope was the same for all wavelengths. Images were recorded with a cooled and amplified CCD color camera (AVT Horn MC 3255).

Eccentric infra-red photorefractometry

Eccentric infra-red photorefractometry is an elegant method for measuring the refractive state of the eye from a distance of up to several meters in non-cooperative subjects (Schaeffel et al. 1987). Multifocal lenses lead to characteristic, ring-like patterns in photorefractive images. An infra-red-sensitive CCD camera (AVT Horn BC6) was used in combination with an infra-red photoretinoscope consisting of four rows of light sources with eccentricities ranging from 5 to 23 mm. To test the adequacy of the method for the detection of multiple focal lengths in animal eyes, we composed a bifocal lens from a 0.5-diopter ophthalmic lens in contact with a larger, 5-diopter lens. With a sheet of white paper representing the retina, this *artificial eye* was video-taped from a distance of 2 m with the retinoscope mounted on a Tamron $F=80$, $f/3.8$ lens.

Patterns in photorefractive images may have other causes than multiple focal lengths (Campbell et al. 1995; Roorda and Campbell 1997). To investigate the origin of the patterns observed in our study, excised fish lenses (blue acara and crucian carp) were suspended by their ligaments in front of a diffusely reflecting, grey surface in H10 medium. Those *semi-artificial eyes* were taped from a distance of 0.7 m with the retinoscope attached to a Minolta $F=135$ mm, $f/2.8$ lens. *Single-pass refractometry* was performed by mounting fish lenses in front of a back-lit slit which was slightly eccentric to the optical axis of the fish lens – camera objective (Tamron) optical system. For in vivo recordings, the retinoscope was attached to a Minolta $F=135$ mm, $f/2.8$ lens and the eyes were video-taped from a distance of 0.7 m (Figs. 6a–f, 7c,d, 8), 0.9 m (Fig. 7b,e,f), or 1.3 m (Fig. 7a).

Results

Ray-tracing

An idealized fish lens free of LSA focuses parallel, monochromatic light onto a narrow retinal area (Fig. 2a). In the presence of LCA, the position of this focal area shifts along the optical axis as a function of wavelength. Therefore, if white light enters the eye, only a narrow band of wavelengths can be in focus on the retina (Fig. 2a). In contrast, the *H. burtoni* lens focuses monochromatic light onto three narrow maxima of light spaced along the optical axis (Fig. 2b). Since the LSA of the *H. burtoni* lens is essentially insensitive to wavelength (Kröger and Campbell 1996), the positions of those focal areas shift along the optical axis as a function of wavelength without notable changes in shape and relative positions. This means that if the distance between lens and retina is fixed, each focal area creates an image at a particular wavelength. If the distance between the lens center and the cone entrance apertures is 2.235 R, there is a focal area for the λ_{max} of each of the three spectral cone types (Fig. 3a). When parallel, white light enters the *H. burtoni* eye, wavelengths at or close to the λ_{max} of the cones are in focus (Fig. 3b).

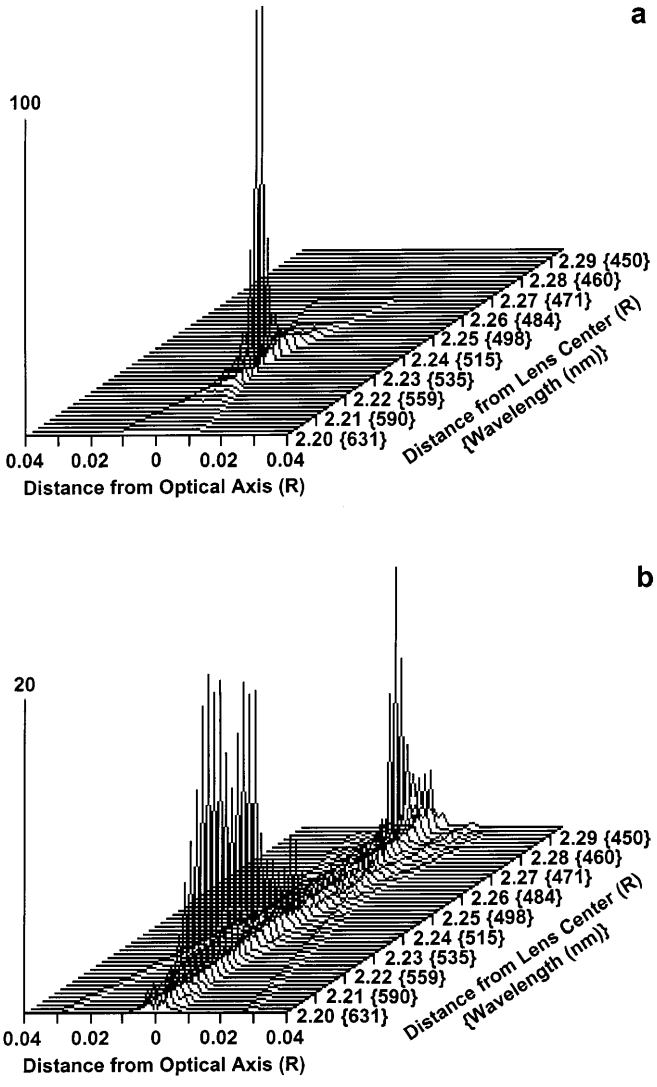

Fig. 2 a The intensity of light (*vertical scale*, arbitrary units) on the retina in the image of a distant point source of monochromatic light was derived by ray-tracing for an idealized fish lens free of LSA with a focal length of 2.235 *R*. Retinal position was changed from 2.200 *R* to 2.295 *R* (depth axis). Since depth of field is short, the light is distributed over large retinal areas if the image is not precisely in focus. Because of LCA, varying the wavelength while keeping the distance between lens and retina fixed has the same effect as varying retinal position in monochromatic light. Assuming that the idealized fish lens has the same amount of LCA as the *H. burtoni* lens (Fig. 1a), the depth scale could be recalibrated to wavelength if the distance between lens and retina is fixed at 2.235 *R* and parallel, white light is focused by the lens. Note that only a narrow band of wavelengths is in focus. **b** The same type of calculation as in **a** was performed using the LSA of the *H. burtoni* lens shown in Fig. 1b. The *H. burtoni* lens creates three images, indicated by maxima of light concentrated within narrow focal areas, at increasing distances from the lens center. Monochromatic light focused at long distances from the lens creates blur-rings if the retina is close to the lens (visible as small, laterally displaced peaks) and vice versa. Since LCA does not affect the shape of LSA of the *H. burtoni* lens (Kröger and Campbell 1996), the depth axis could be recalibrated to wavelength as in **a**. If white light is imaged by the lens, each well-focused image at a wavelength close to the λ_{max} of a spectral cone type is overlayed with blur created by zones of the lens focusing other wavelengths

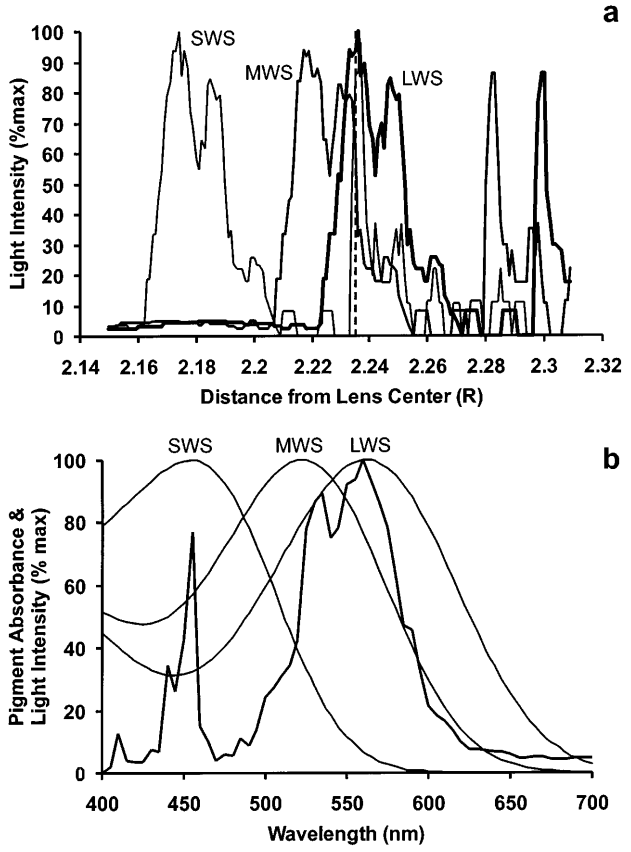

Fig. 3 a The optimum position of the retina was found by calculating relative light intensities within the central retinal bin (diameter = 0.0015 *R*) as a function of the distance between lens and retina at the λ_{max} of the three spectral cone types in the *H. burtoni* retina. At about 2.235 *R* from the lens center (*dashed vertical line*), there is a focal area at the λ_{max} of each spectral cone type. **b** Spectral distribution of light from a distant source of white light focused on the central bin with the retina at a distance from the lens of 2.235 *R*. Thin traces are nomograms of cone pigment absorbance spectra (Fernald and Liebman 1980). Wavelengths at or close to the λ_{max} of the three spectral cone types are focused on the retina, while other wavelengths are out of focus (see also Fig. 2b)

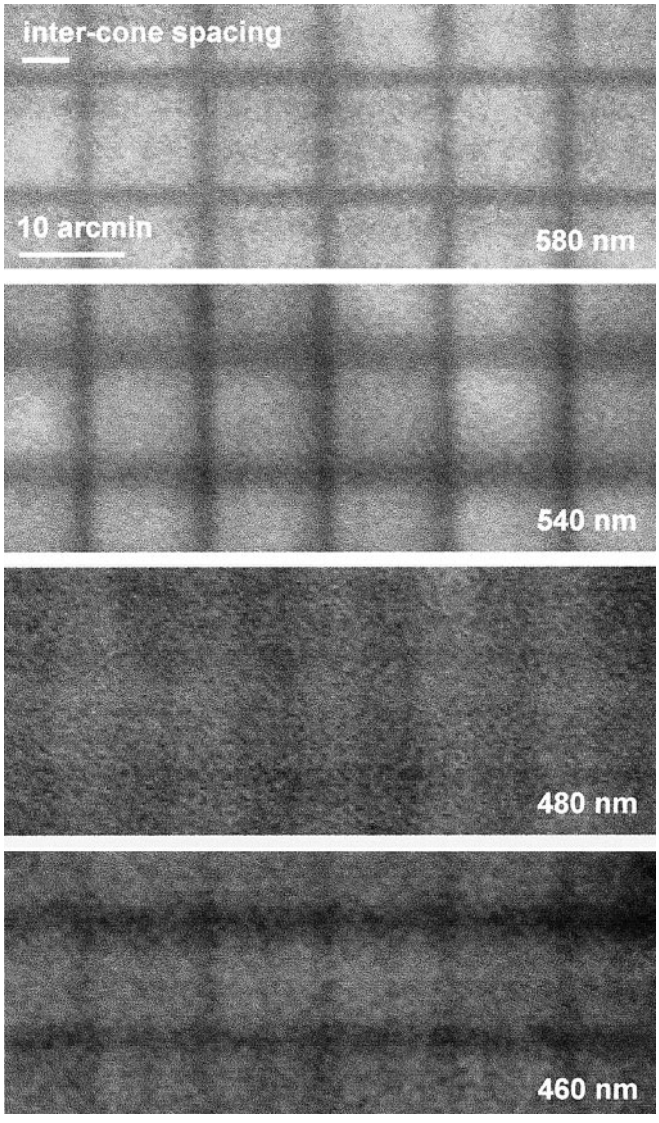

Fig. 4 Images of a fine copper grid as used to mount specimens for electron microscopy were taken through an *A. pulcher* lens with a radius of 1.5 mm at wavelengths close to the wavelengths of maximum absorbance of the three spectral cone types. The focal setting of the microscope used for observation was identical for all images. The *A. pulcher* lens created an image at the λ_{max} of each spectral cone type in spite of 9.2 diopters difference in refractive power between 460 and 580 nm. The faint pattern at 480 nm is most likely due to a reversal of modulation transfer caused by defocus (spurious resolution), since it is opposite in spatial phase to the patterns at the other wavelengths. A very faint pattern of opposite phase was also visible at 460 nm

Fish lens imagery

In a cichlid lens with a radius of 1.5 mm, the difference in image position is 75 μm between 460 and 540 nm, and 22 μm between 540 and 580 nm (Kröger and Campbell 1996). In spite of this substantial expected difference in image positions, the *A. pulcher* lens created well-focused images at the λ_{max} of each spectral cone type in a single plane (Fig. 4). There was no image at 480 nm (Fig. 4), indicating that the image at 460 nm was not due to depth of field of the fish lens-microscope system.

Photorefractometry

When photorefractometry was applied on the artificial eye with two concentric lenticular zones of different refractive power, the reflexes split up into two rings (Fig. 5a). Similar, although more numerous, rings were present in photorefractive images obtained from semi-artificial eyes (Fig. 5b) and by single-pass refractometry (Fig. 5c). Rings were also present in images obtained in vivo from the eyes of *H. burtoni*, *A. pulcher* and other fishes with well-developed color vision (Fig. 6a–f). They have been observed in additional fish species, including marine teleost and elasmobranch species (Howland et al. 1992; Cronin 1998). Numbers and positions of the rings were constant within each species and independent of

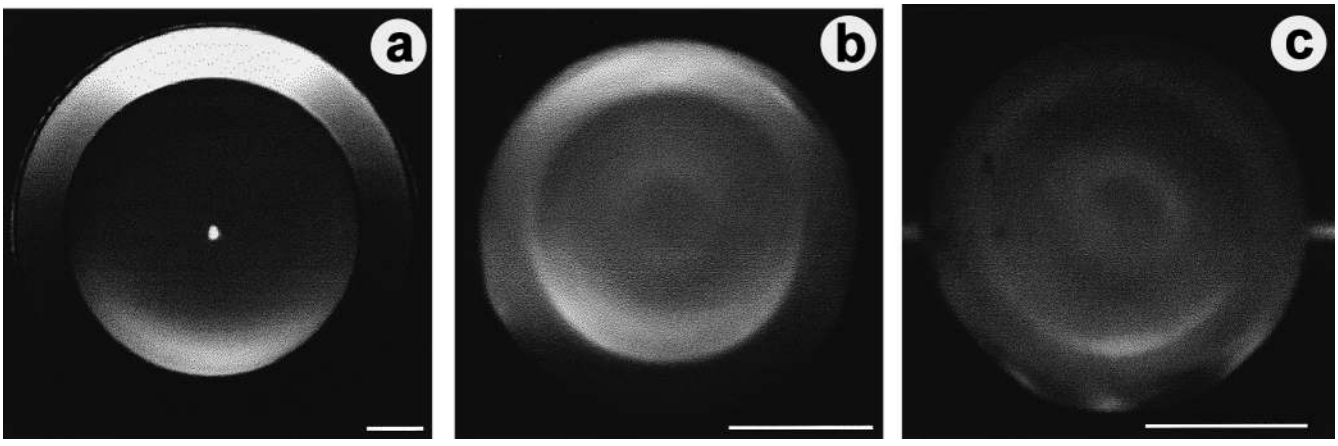

Fig. 5 Photorefractive images obtained from an artificial eye with a bifocal lens with concentric zones of different refractive power (**a**), from a semi-artificial eye consisting of an *A. pulcher* lens and a flat gray plastic sheet representing the retina (**b**), and by single-pass refractometry of an *A. pulcher* lens (**c**). Multiple focal lengths result in ring-like patterns. Scale bars: 1 cm (**a**), 1 mm (**b**,**c**)

the axis that was refracted (Fig. 7). Rings were also present in photorefractive images of horses, cats, and nocturnal geckos (Fig. 8a–c). The absence of rings in the pupils of diurnal geckos, dogs, and humans (Fig. 8d–f) suggests that the lenses of those species have no discrete multiple focal lengths.

Fig. 6a–f Photorefractive images obtained in vivo from various species of fish with well-developed color vision and pupils unresponsive to light. Multifocal lenses appear to be widespread among fishes since rings were found in all species investigated. Scale bars = 5 mm

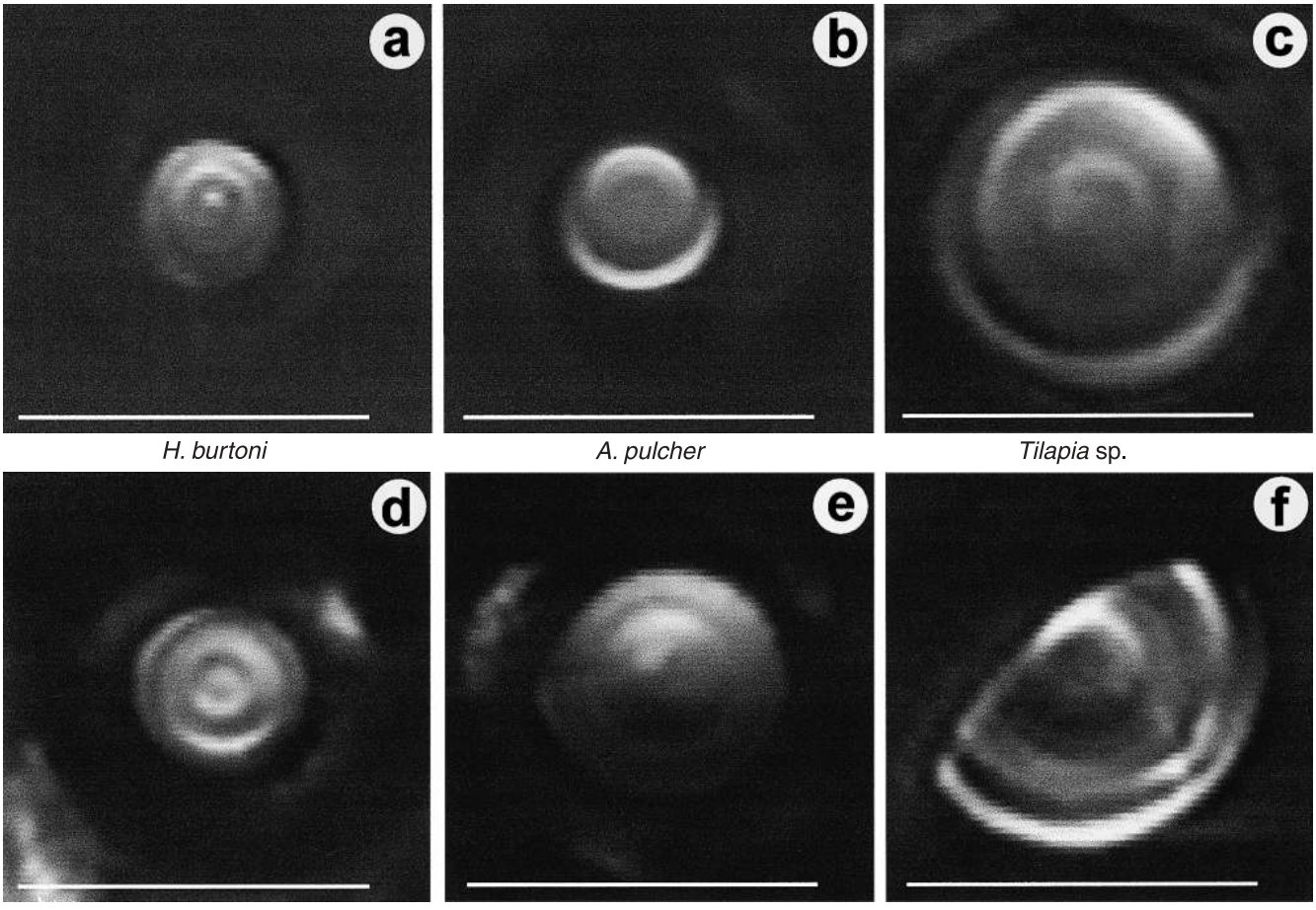

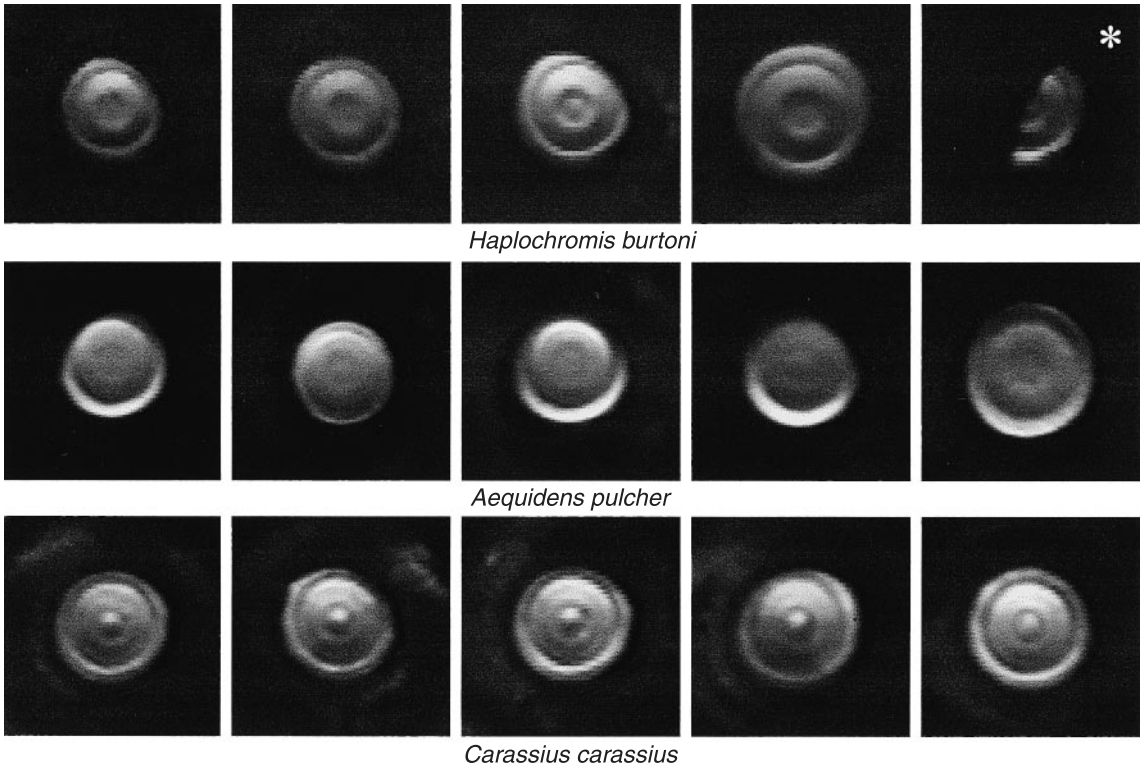

Fig. 7 Photorefractive images from different individuals of three species of fish. The numbers and positions of the rings in photorefractive reflexes show little intra-specific variation, despite differences in eye size. One example of an oblique refraction (*asterisk*) is shown to demonstrate that the presence of rings is independent of the axis of refraction. The zones of different refractive power vary in brightness between animals of the same species since refractive state was not controlled. Scale bar = 1 mm

Discussion

Ray-tracing and lens imagery

Indirect modeling of lens performance and direct demonstration of image positions both indicate that the spacings between the focal lengths of the lens match the amount of LCA present for the retinal complement of spectral cone types in the eyes of *H. burtoni* and *A. pulcher*. The peculiar shape of the LSA of the cichlid lens thus serves to focus several wavelengths on the retina, as is illustrated in Fig. 9. In previous work on the lens of the rainbow trout, which was found to have multiple focal lengths using methods different from ours, it was assumed that chromatic and monochromatic aberrations could not interact to correct each other (Jagger 1996, 1997; Jagger and Sands 1996).

Fernald and Wright (1985b) used 2.252 *R* as the focal length of the *H. burtoni* lens and found that the image of a distant object fell within the photoreceptor layer. Furthermore, cichlids and many other fish species accommodate by adjusting lens position with respect to the retinal plane (Sivak 1975; Fernald and Wright 1985a). It therefore seems reasonable to assume that the entrance aperture of the cones is at 2.235 *R* when a fish views distant objects. Our ray-tracing calculations do not account for directionality of photoreceptor sensitivity (Enoch and Lakshminarayanan 1991), radial defects within the lens (Jagger 1997), and diffraction. Image quality cannot be derived in detail from ray-tracing model calculations. It was therefore necessary to demonstrate with direct methods that the cichlid lens can create well-focused images at the λ_{max} of the cones.

Photorefractions

Prominent rings in photorefractive images appear to be indicative of multifocal lenses. To verify this conclusion, we investigated a variety of other possible causes of patterned photorefractive images. Lenticular opacities could not be detected by slit-lamp examinations of *H. burtoni* eyes (Kröger et al. 1994) and traditional "zones of discontinuity" in the lens (Brown et al. 1988) do not give rise to such rings, since they are not visible in the human eye. A retinal origin of the rings can be excluded, since photorefractive images obtained from semi-artificial eyes were almost indistinguishable from those observed in live animals. In single-pass photorefractions, the rings were as well defined as in images obtained from semi-artificial eyes or in vivo measurements (Figs. 5, 6). It is thus highly unlikely that the rings observed in fish eyes are caused by internal reflections within the lens. Optical aberrations of the eye other than spherical aberration can also lead to patterns in photorefractive

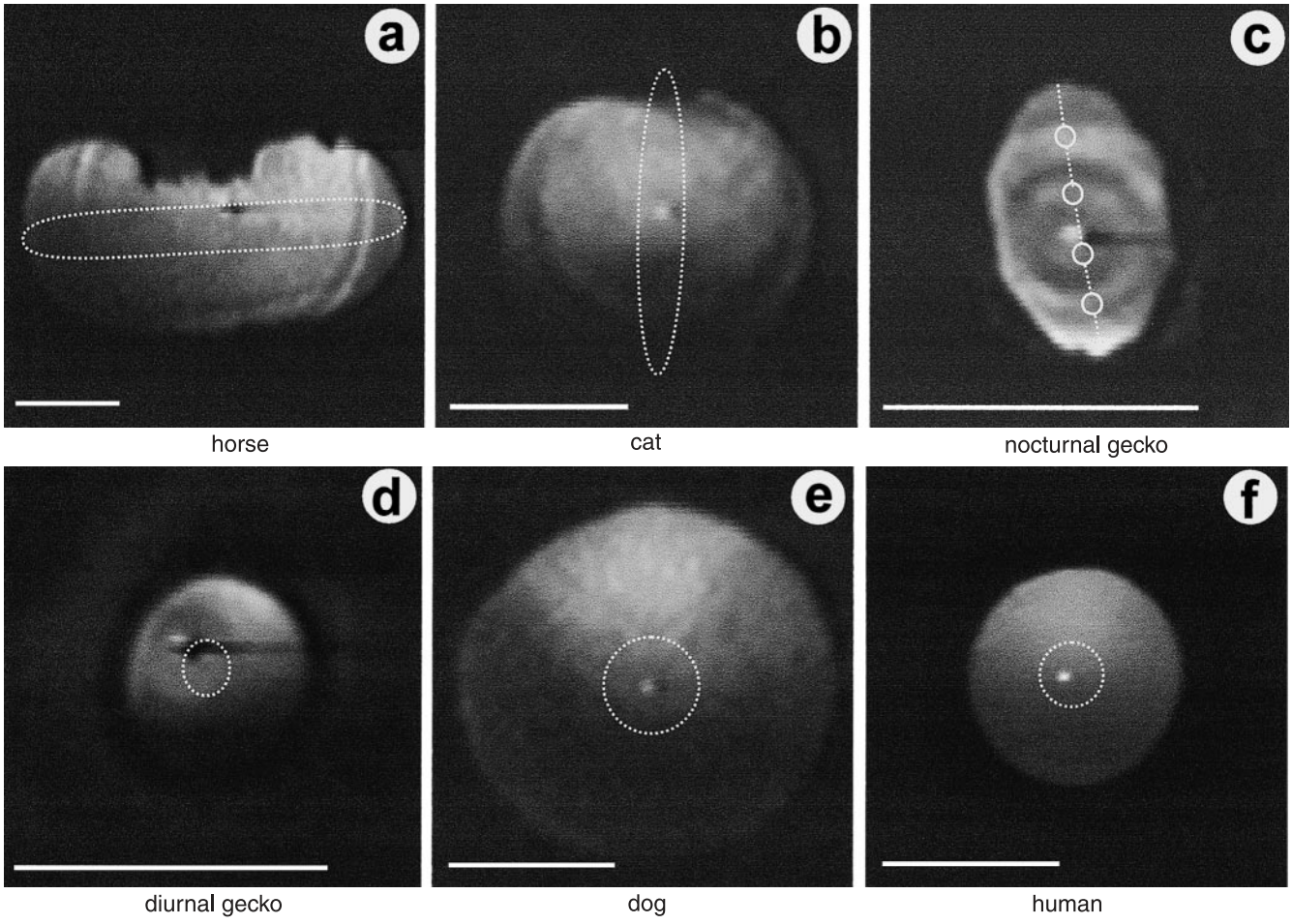

Fig. 8 Rings indicative for multiple focal lengths are also present in photorefractive images obtained from terrestrial animals which have slit pupils (**a,b**) or multiple pupillary openings in bright light (**c**). In species with circular pupils centered on the optical axis, the reflexes have smooth distributions of light indicative for optical systems with single focal lengths or smoothly varying spherical aberration (**d–f**). Approximate light-adapted pupil shapes are shown as *dotted lines*. All mammals were young adults. The *dark*, *horizontal stripes* visible in the gecko pupils are artifacts due to overload of the video system by bright Purkinje reflexes. Nocturnal gecko: *Homopholis wahlbergi*, diurnal gecko: *Phelsuma madagascariensis*. Scale bars = 5 mm

images (Campbell et al. 1995; Roorda and Campbell 1997). However, the numbers and positions of the rings were independent of the axis that was refracted in both isolated lenses and live fish. The rings must therefore originate from a symmetrical aberration of the lens. Finally, the numbers and positions of the rings were constant within each species and independent of the size of an individual and its eye (Fig. 7), but varied between species (Figs. 6, 8), suggesting that they are due to specific optical adaptations.

Lens and eye design

The optical properties of powerful crystalline lenses are very sensitive to the precise gradient of refractive index (e.g., Campbell and Hughes 1981; Jagger 1992; Kröger et al. 1994). Although it is known that the gradient in the fish lens is continually maintained despite significant growth (Fernald and Wright 1985b) it is not known how the index profile is produced developmentally. Our new finding that multifocal lenses necessitate the independent regulation of the refractive gradient of several concentric zones within the lens adds yet another constraint on the development and growth of gradient index lenses. This is a particularly vexing problem because in multifocal lenses, peripheral zones must influence the optics of more central zones. This fine tuning of the optical properties of the lens suggests that a sophisticated feedback mechanism may be responsible for maintenance of suitable image quality.

The fundamental constraint on lens development is that chromatic aberration depends on the properties of the lens material itself. Although some fish species, including *H. burtoni*, have lower chromatic aberration than predicted from the average dispersion of ocular media (Kröger 1992; Kröger and Campbell 1996), achromatic eyes appear to be impossible in vertebrates since the animals are limited to the use of proteins in aqueous solution for this function. If the pupillary opening is small and depth of field correspondingly long, this problem is not severe. Furthermore, some

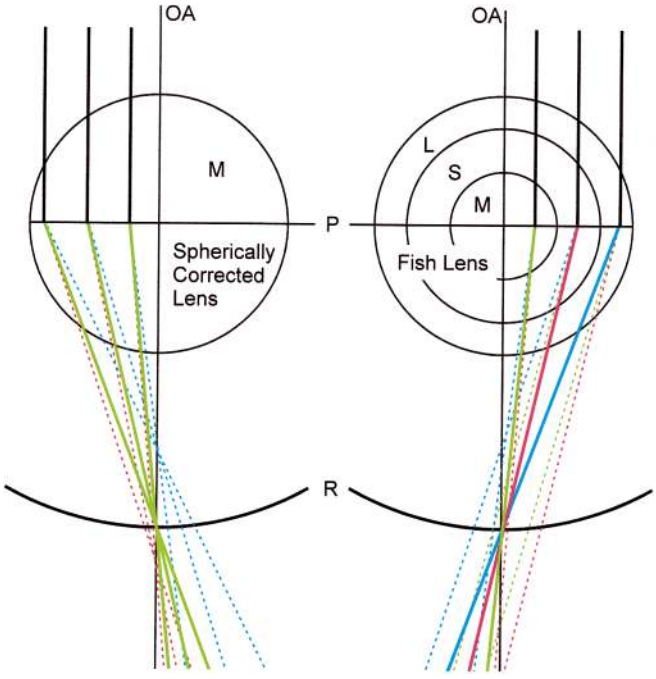

Fig. 9 Schematic representation of image formation by an idealized fish lens that is perfectly corrected for spherical aberration (**a**) and the lens of a cichlid fish consisting of concentric shells of different focal lengths (**b**). The idealized lens creates a well-focused image only at the λ_{max} of a single spectral cone type, in this example the middle-wave-sensitive cones. The images are severely defocused for the remaining classes of cone. Conversely, the fish lens creates an image at the λ_{max} of each cone type. Rays of light not in focus constitute blur which reduces image contrast at high spatial frequencies. Image formation by a fish lens is more complicated than shown here, since peripheral shells influence the optical properties of central zones. LCA has been exaggerated to improve the clarity of the diagram. *OA* optical axis, *P* principal plane, *R* retina; *L*, *M*, *S* long, medium, short focal length

species, including humans which have only LWS and MWS cones in the fovea, use only a limited part of the visual spectrum for high-resolution vision. In eyes with large pupils and cone pigments of wide spectral separation, however, multifocal optics may be the only solution to generate images of sufficient detail for all cone types.

Multifocal optical systems improve spatial resolution of color vision at the cost of image contrast, which is reduced at high spatial frequencies by blur from out-of-focus images. Chromatic defocus is particularly severe if animals are capable of UV-vision. At the short-wave end of the spectrum, dispersion (and thus LCA) rises almost exponentially (e.g., Longhurst 1973; see also Fig. 1a). If none of the focal lengths of the lens is tuned to the absorbance of the UVS cones, image quality in the UV range is seriously reduced by chromatic defocus. Conversely, contrast is low if the lens has a focal length for each cone type in multichromatic species with widely spaced visual pigments. In many species, this reduction in contrast appears to be outweighed by the gain in spatial resolution of color vision.

The advantage of multifocal lenses is evident if the animals have color vision. However, animals with monochromatic visual systems may also benefit from residual LSA. If depth of field is as short as in the typical fish eye, small objects easily blend into the background if they reflect or emit only wavelengths not precisely in focus. If the lens is well corrected for spherical aberration and only high spatial frequencies are considered, effective spectral tuning of the visual system is thus considerably narrower than photopigment absorbance would suggest (see Fig. 2a). Residual LSA increases depth of field and thus reduces the defocusing effect of LCA. Perfect correction of spherical aberration therefore may not to be the optimum solution even in many monochromatic species.

In terrestrial eyes, the refractive power of the cornea, which resembles an air-water interface, is substantial. Since the proteins in the fish lens have higher dispersion than water (Sivak and Mandelman 1982), total LCA is somewhat lower in a terrestrial eye with the same power as a fish eye. However, the eyes of nocturnal animals, like the cat, for instance, have even smaller *f*-numbers than the *H. burtoni* eye (Martin 1983), and thus shorter depth of field. Furthermore, a large eye can have higher angular resolution than a small eye, since maximum absolute cone density is limited by the wave-guiding properties of photoreceptors (Snyder 1975). Since the size of the blur circle due to LCA is proportional to focal length, degradation of image quality relative to the smallest possible cone spacing increases with eye size. Chromatic defocus is thus a considerable problem in terrestrial species which have large eyes with small *f*-numbers and high retinal resolution. Accordingly, some species also appear to have developed eyes with multiple focal lengths (Fig. 8). The functional significance of multifocal lenses is strikingly demonstrated by the differences in eye design within the Gekkonidae: nocturnal geckos have eyes with small *f*-numbers and multiple focal lengths. As a result of smaller pupil size, depth of field is longer in diurnal geckos and multifocal lenses are absent.

Pupil shape

A multifocal lens is most useful if its zones of different refractive power are not occluded by a mobile iris and therefore can be used at all light levels. In the fish eyes shown in Fig. 6, the pupil does not constrict in response to light. Horses and cats have horizontal and vertical slit pupils, respectively, which allow almost the full diameter of the lens to participate in the imaging process irrespective of the state of pupil constriction (Fig. 8a, b). Under moderate light levels, the pupil of nocturnal geckos is similar to a partially closed slit pupil. In bright light, the pupil constricts to two pairs of holes symmetrical to the optical axis in about the dorso-ventral meridian (Fig. 8c). An image can be generated for each of the two main spectral cone types (Loew et al. 1996) through a corresponding pair of pupillary openings, conserving short depth of field that may be important to

obtain depth cues in monocular vision (Murphy and Howland 1986). Pupillary specializations are absent in species which show no rings in the photorefractive reflexes and therefore are likely to have eyes with smoothly varying spherical aberration (Fig. 8d–f). The presence of multifocal lenses thus provides a new functional interpretation of slit pupils and some other pupil shapes which allow the zones of different refractive power of the lens to be used for imaging irrespective of light level.

Acknowledgements The authors thank A. Mack, M. Ott, U. Schrodt, W. Vogel, and the Wilhelma Zoological-Botanical Garden of Stuttgart, Germany, for access to their animals, M. Ott for help with the photorefractions, B. Hirt for assistance in taking images through fish lenses, H. Howland, M. Land, and F. Schaeffel for suggesting critical experiments, and T. Cronin, R. Douglas, M. Land, and A. Roorda for useful discussion and comments on the manuscript. Supported by DFG, Germany, Wa 348/17 (R.H.H.K., H.-J.W.), NSERC, Canada, URF, and Operating Grant (M.C.W.C.) and NIH, U.S.A., EY 05051 (R.D.F.).

References

Axelrod D, Lerner D, Sands PJ (1988) Refractive index within the lens of a goldfish eye determined from the paths of thin laser beams. Vision Res 28: 57–65

Bowmaker J (1995) The visual pigments of fish. Prog Retinal Eye Res 15: 1–31

Brown NA, Sparrow JM, Bron AJ (1988) Central compaction in the process of lens growth as indicated by lamellar cataract. Br J Opthalmol 72: 538–544

Campbell MCW, Hughes A (1981) An analytic, gradient index schematic lens and eye for the rat which predicts aberrations for finite pupils. Vision Res 21: 1129–1148

Campbell MCW, Bobier WR, Roorda A (1995) Effect of monochromatic aberrations on photorefractive patterns. J Opt Soc Am A 12: 1637–1646

Eberle H (1968) Zapfenbau, Zapfenlänge und chromatische Aberration im Auge von *Lebistes reticulatus* Peters (Guppy). Zool Jahrb Abt Allg Zool Physiol Tiere 74: 121–154

Enoch JM, Lakshminarayanan V (1991) Retinal fibre optics. In: Charman WN (ed) Visual optics and instrumentation. MacMillan, London, pp 280–309

Fernald RD (1981) Chromatic organization of a cichlid fish retina. Vision Res 21: 1749–1753

Fernald RD (1983) Neural basis of visual pattern recognition. In: Ewert J-P, Capranica RR, Ingle DJ (eds) Advances in vertebrate neuroethology. Plenum Press, New York, pp 569–580

Fernald RD, Liebman P (1980) Visual receptor pigments in the African cichlid fish, *Haplochromis burtoni*. Vision Res 20: 857–864

Fernald RD, Wright S (1985a) Growth of the visual system of the African cichlid fish, *Haplochromis burtoni*: accommodation. Vision Res 25: 163–170

Fernald RD, Wright S (1985b) Growth of the visual system of the African cichlid fish, *Haplochromis burtoni*: optics. Vision Res 25: 155–161

He S, MacLeod DIA (1998) Local nonlinearity in S-cones and their estimated light-collecting apertures. Vision Res 38: 1001–1006

Hikida M, Iwata S (1987) In vitro subacute cataractogenic study in rainbow trout lenses. J Pharmacobiodyn 10: 443–448

Howland CH, Murphy CJ, McCosker JE (1992) Detection of eyeshine by flashlight fishes of the family Anomalopidae. Vision Res 32: 765–769

Jagger WS (1992) The optics of the spherical fish lens. Vision Res 32: 1271–1284

Jagger WS (1996) Image formation by the crystalline lens and eye of the rainbow trout. Vision Res 36: 2641–2655

Jagger WS (1997) Chromatic and monochromatic optical resolution in the rainbow trout. Vision Res 37: 1249–1254

Jagger WS, Sands PJ (1996) A wide-angle gradient index optical model of the crystalline lens and eye of the rainbow trout. Vision Res 36: 2623–2639

Kröger RHH (1992) Methods to estimate dispersion in vertebrate ocular media. J Opt Soc Am A 9: 1486–1490

Kröger RHH, Campbell MCW (1996) Dispersion and longitudinal chromatic aberration of the crystalline lens of the African cichlid fish *Haplochromis burtoni*. J Opt Soc Am A 13: 2341–2347

Kröger RHH, Fernald RD (1994) Regulation of eye growth in the African cichlid fish *Haplochromis burtoni*. Vision Res 34: 1807–1814

Kröger RHH, Wagner H-J (1996) The eye of the blue acara (*Aequidens pulcher*, Cichlidae) grows to compensate for defocus due to chromatic aberration. J Comp Physiol A 179: 837–842

Kröger RHH, Campbell MCW, Munger R, Fernald RD (1994) Refractive index distribution and spherical aberration in the crystalline lens of the African cichlid fish *Haplochromis burtoni*. Vision Res 34: 1815–1822

Kröger RHH, Bowmaker JK, Wagner H-J (1999) Morphological changes in the retina of *A pulcher* (Cichlidae) after rearing in monochromatic light. Vision Res (in press)

Loew ER, Govardovskii VI, Röhlich P, Szél Á (1996) Microspectrophotometric and immunocytochemical identification of ultraviolet photoreceptors in geckos. Vis Neurosci 13: 247–256

Longhurst RS (1973) Geometrical and physical optics. Longman, London

Martin GR (1983) Schematic eye models in vertebrates. In: Ottoson D (ed) Progress in sensory physiology. Springer, Berlin Heidelberg New York, pp 43–81

Matthiessen L (1882) Über die Beziehungen, welche zwischen dem Brechungsindex des Kernzentrums der Krystalllinse und den Dimensionen des Auges bestehen. Pfluegers Arch 27: 510–523

Matthiessen L (1886) Über den physikalisch-optischen Bau des Auges der Cetaceen und der Fische. Pfluegers Arch 38: 521–528

Murphy CJ, Howland HC (1986) On the gekko pupil and Scheiner's disc. Vision Res 26: 815–817

Pierscionek BK, Augusteyn RC (1991) Structure/function relationship between optics and biochemistry of the lens. Lens Eye Toxic Res 8: 229–243

Pierscionek BK, Chan DY (1989) Refractive index gradient of human lenses Optom Vis Sci 66: 822–829

Roorda A, Campbell MCW (1997) Slope-based eccentric photorefraction: theoretical analysis of different light source configurations and effects of ocular aberrations. J Opt Soc Am A 14: 2547–2556

Schaeffel F, Farkas L, Howland HC (1987) Infrared photoretinoscope. Appl Opt 26: 1505–1509

Sivak JG (1975) Accommodative mechanisms in aquatic vertebrates. In: Ali MA (ed) Vision in fishes. Plenum Press, New York, pp 289–297

Sivak JG (1991) Shape and focal properties of the cephalopod ocular lens. Can J Zool 69: 2501–2506

Sivak JG, Kreuzer RO (1983) Spherical aberration of the crystalline lens. Vision Res 23: 59–70

Sivak JG, Mandelman T (1982) Chromatic dispersion of the ocular media. Vision Res 22: 997–1003

Sivak JG, West JA, Campbell MCW (1994) Growth and optical development of the ocular lens of the squid (*Sepioteuthis lessoniana*). Vision Res 34: 2177–2187

Snyder AW (1975) Photoreceptor optics – theoretical principles. In: Snyder AW, Menzel R (eds) Photoreceptor optics. Springer, Berlin Heidelberg New York

Sroczynski S (1976) Die chromatische Aberration der Augenlinse der Regenbogenforelle (*Salmo gairdneri* Rich.). Zool Jahrb Abt Allg Zool Physiol Tiere 80: 432–450